Electrochemistry Communications 109 (2019) 106580

Contents lists available at ScienceDirect

Electrochemistry Communications

journal homepage: www.elsevier.com/locate/elecom

Copper electrodeposition onto zinc for the synthesis of kesterite Cu_2ZnSnS_4 from a Mo/Zn/Cu/Sn precursor stack

Gabriele Panzeri[a], Ruben Dell'Oro[a], Vanira Trifiletti[b], Jacopo Parravicini[b], Maurizio Acciarri[b], Simona Binetti[b], Luca Magagnin[a,*]

[a] *Department of Chemistry, Materials and Chemical Engineering Giulio Natta Politecnico di Milano, 20131 Milano, Italy*
[b] *Department of Materials Science e Solar Energy Research Center (MIB-SOLAR), University of Milano-Bicocca, 20125 Milano, Italy*

ARTICLE INFO

Keywords:
Organic solution
Ethylene glycol
Diethanolamine
Chloride-free
CZTS

ABSTRACT

A chloride-free solution based on ethylene glycol was shown to be suitable for the electrodeposition of copper onto zinc, allowing the fabrication of a Mo/Zn/Cu/Sn metallic precursor stack. The addition of diethanolamine (DEA) played an essential role in minimizing displacement reactions by shifting copper reduction towards a more negative potential. The electrochemical behavior of copper species with and without DEA was studied by cyclic voltammetry, and subsequently confirmed by displacement reaction assessment (OCV and ICP-OES measurements). The metallic stack was characterized by SEM and AFM, showing the effectiveness of the copper plating solution. Reactive annealing was carried out in a tubular furnace to obtain the CZTS kesterite semiconductor, as confirmed by XRD and Raman spectroscopy.

1. Introduction

Cu_2ZnSnS_4 (CZTS) thin film technology has been widely investigated for photoconversion devices in the last few decades. The employment of earth-abundant elements, suitable optical properties such as an energy bandgap of 1.4–1.5 eV and a relatively high absorption coefficient ($\alpha > 10^4\ cm^{-1}$) are the prerequisites for potential low-cost and high-efficiency devices [1,2]. Electrodeposition is one of the most attractive fabrication routes since it is a large-area and low-cost process, and because the difference in power conversion efficiency compared with CZTS-based devices from vacuum-based techniques, highly controlled yet expensive, is not significant [2–4]. Considering the electrodeposition-annealing fabrication route, the best solar cell efficiencies are obtained through the stacked elemental layer (SEL) approach, which allows easy tuning of the precursor stack composition by changing the thickness of the single layers [5,6]. The stacked layer approach has been one of the most investigated fabrication routes, despite the simpler experimental configuration for the case of co-electrodeposition of Cu-Zn-Sn precursors. The latter indeed imposes more constraints on bath chemistry along with less control on composition uniformity, especially for large areas [6]. On the other hand, the electrochemical SEL method has limitations due to the difference in the reduction potentials of the elements [6]. The electrochemical synthesis of CZTS was firstly proposed by Scragg et al. [7] using a metal layer sequence: firstly depositing the noblest one ($Cu^{2+} + 2e^- \rightarrow Cu^0$, $E^0_{Cu} = +0.34$ V vs RHE) followed by tin ($Sn^{2+} + 2e^- \rightarrow Sn^0$, $E^0_{Sn} = -0.13$ V vs RHE) and zinc layers ($Zn^{2+} + 2e^- \rightarrow Zn^0$, $E^0_{Zn} = -0.76$ V vs RHE), with a progressive decrease in the reduction potential of the layers (Cu/Sn/Zn) [6,8]. Since the difference in reduction potential between copper and tin is quite low, a limited or negligible displacement reaction is observed when electrodepositing copper onto a tin substrate. This allows the exploitation of a number of different sequence combinations such as Cu/Sn/Cu/Zn [9] and Sn/Cu/Zn [10], although one study has also shown the feasibility of a Cu/Zn/Sn stack [5]. The main limitation thus comes from the zinc layer because of its low nobility, the large difference with the reduction potentials of copper and tin making it impossible to carry out electrodeposition on top of it without a significant galvanic displacement reaction, leading to the complete dissolution of zinc in the bath and the reduction of copper or tin metallic ions at the zinc surface. In the case of copper displacement onto zinc, the reaction may be fast, involving the complete conversion of the zinc layer in a few seconds, with an evident loss of compositional control. Recently a Zn/Cu/Sn stack sequence has been fabricated by electrochemical means using a cyanide complexed bath [11], reducing the difference in the reduction potential of the metallic species, and by compensating the displacement loss by adding zinc precursor salts to the copper plating bath [11]. Araki et al. investigated several stack combinations by means of evaporation,

---

[*] Corresponding author.
E-mail address: luca.magagnin@polimi.it (L. Magagnin).

https://doi.org/10.1016/j.elecom.2019.106580
Received 13 August 2019; Received in revised form 4 October 2019; Accepted 22 October 2019

showing a significant dependence of solar cell efficiency on the metallic stack layer sequence [12]: the best results were obtained when copper and tin layers were adjacent, probably due to the formation of intermediate Cu-Sn sulfide, then transformed into CZTS. Among the combinations left, Mo/Zn/Cu/Sn was identified as the most promising, with a significant efficiency increase compared to conventional Mo/Cu/Sn/Zn with the same stack composition, stack layer fabrication parameters, reactive annealing conditions, and solar cell finalization layers [12]. The aim of the present work is to provide a novel electrochemical fabrication route for the Zn/Cu/Sn precursor stack, involving the use of a non-aqueous plating solution for the copper layer. The use of an organic solution is a possible alternative to avoid aqueous chemistry for reactive substrates [13,14]. Acting on the complexation of the metallic ions in solution, the difference in the reduction potentials of the species involved in the process can be reduced, minimizing and/or controlling the displacement reactions, as demonstrated in the present work.

2. Experimental

Anhydrous ethylene glycol (EG) (99.8% Sigma Aldrich), copper acetate (99.99% Sigma Aldrich), sodium acetate (99% Sigma Aldrich), diethanolamine (DEA) (98% Sigma Aldrich) and dimethylamine borane complex (97% Fluka) were used as received. Ethylene glycol was heated up to 70 °C followed by the addition of copper precursor salt (0.05 M) and sodium acetate (1 M). Once completely dissolved, DEA (0.8 M) was added and, finally, dimethylamine borane complex (0.1 g/L). The bath (100 ml) was kept at 70 °C during solution preparation and testing. Cyclic voltammetry (CV) was carried out using an inert working electrode (WE), namely a glassy carbon rod of 3 mm diameter, while graphite and platinum wire were used as counter-electrode (CE) and quasi-reference electrode (QRE), respectively. For the galvanic displacement investigation, a similar three-electrodes setup was used but zinc-coated (250 nm thick) molybdenum-sputtered soda lime glass (SLG/Mo/Zn) was used as WE. Preliminary investigations of copper deposition were carried out in a 33 ml hull cell (Tenori Hull cell, YAMAMOTO-MS). Inductively coupled plasma–optical emission spectrometry (ICP-OES) (Perking Elmer Optima 8300) was used to analyze the Mo/Zn sample after immersion for 10 s in the copper plating solution, with no applied bias; the sample was mineralized by microwave-assisted acid etching before the analysis. For the fabrication of the Zn/Cu/Sn metallic precursor stack ($1.5 \times 1.5\ \mathrm{cm}^2$ film area), galvanostatic deposition was considered for all layers. The zinc layer was electrodeposited from a commercially available acidic solution based on sulfate chemistry (TECNOZINC, Tecnochimica) with a current density of $-10\ \mathrm{mA/cm}^2$ for 60 s, keeping the bath temperature at $T = 25$ °C under stirring conditions. The second step involved the electrodeposition of copper from the aforementioned organic solution, imposing a current density of $-2\ \mathrm{mA/cm}^2$ for 16 min at a bath temperature of $T = 70$ °C, under quiescent conditions. Finally, the tin layer was electrodeposited using an aqueous solution comprising 1 M methanesulfonic acid, 0.05 M tin methanesulfonate and 0.1%v. of EMPIGEN BB at a deposition current of $-20\ \mathrm{mA/cm}^2$ for 16 s at bath temperature of $T = 25$ °C under vigorous stirring, based on previous reports [5,9]. The precursor layer was soft annealed in a tubular furnace at 350 °C for 30 min (ramp 10 °C/min) under a nitrogen atmosphere, followed by reactive annealing in a sulfur atmosphere at 580 °C for 10 min at 0.3 bar in a graphite box (steady Ar background atmosphere). Morphological and compositional analyses were carried out by scanning electron microscopy (SEM) (Zeiss EVO 50 EP and Zeiss FEG Gemini 500), atomic force microscopy (AFM) (NT-MDT SOLVER PRO) and electron dispersive spectroscopy (EDS) (Oxford instruments INCA x-sight detector and QUANTAX 4000). Raman measurements were carried out at room temperature with a micro-Raman system (Jasco Ventuno) in backscattering configuration and a He-Ne laser ($\lambda = 632.8$ nm).

3. Results and discussion

3.1. Bath formulation

Since zinc has low nobility, the copper plating bath has to be carefully chosen to minimize displacement reactions, or at least reducing their kinetics. An organic solution was selected to avoid any effect due to aqueous solution pH, since zinc does not have an immunity region at 0 V vs RHE. To further minimize the interaction between the substrate and the solution, chlorides were discarded due to their intrinsic aggressiveness. In addition, a strong copper complexing agent, an amine [15,16], was considered to be a good candidate to reduce the driving force of the displacement reaction. The solution was designed in the light of our previous experience with chloride-free solutions based on ethylene glycol [17]. Due to the relatively large hindrance of acetate anions, a supporting electrolyte (1 M sodium acetate) was necessary to guarantee sufficient ionic conductivity to carry out electrodeposition homogeneously. Ethylene glycol containing 0.05 M copper acetate and the respective sodium salts resulted in a conductivity of 2.4 mS/cm at 25 °C. The addition of 0.8 M DEA clearly increased the overall viscosity of the solution with a consequent decrease in the ionic conductivity to 2.04 mS/cm at 25 °C. However, this reduction was not detrimental to the displacement reaction, since a lower ionic conductivity would in principle limit the transport of copper species towards the electrode surface, thus reducing the displacement kinetics.

3.2. Electrochemical investigation

Cyclic voltammetry analysis was carried out mainly to assess the suitability of the organic solution for the electrodeposition of copper and most importantly to observe the effect of DEA on the reduction potential of copper. Divalent copper species dissolved in EG showed clear electrochemical activity: during the forward scan, the first reduction peak represents the reduction to Cu(I) at −0.28 V vs Pt followed by a second one, at −0.5 V vs Pt, corresponding to reduction to the metallic state Cu(0) (Fig. 1a). With the addition of DEA, the electrochemical behavior changed significantly, showing an irregular broad peak with a minimum at −0.49 V vs Pt, probably related to the presence of DEA and/or a reaction involving its complexes. Most importantly, the copper reduction peak was shifted towards more negative potentials at −0.99 V vs Pt (Fig. 1a), suggesting the possibility of a lower driving force for the displacement reaction with zinc, dependent on the difference in reduction potentials of the two species considered. As a drawback, the addition of DEA also resulted in a narrower electrochemical window with the copper reduction peak close to the hydrogen evolution resulting from organic solvent degradation. This effect is demonstrated by the anodic peaks of the two curves, which in the case of the DEA-containing solution was smaller, despite the higher charge passed during the cathodic scan at a fixed potential interval.

Displacement evaluation was carried out by monitoring the open circuit voltage of the zinc-coated (250 nm) molybdenum substrate upon immersion in the non-aqueous copper solution. The difference in nobility between copper and zinc would result in a galvanic displacement reaction where the zinc dissolves into the solution and copper is reduced at the surface electrode. The immersion potential of the zinc substrate was thus expected to increase as the reaction goes on, in agreement with the progressive replacement of zinc. The experiment did indeed show that the immersion potential of zinc increases after an initial plateau and stabilizes at a more positive potential value when most of the surface atoms have been displaced, i.e. copper atoms cover most of the working electrode area (Fig. 1b). During the initial plateau, whose extent in time is related to the displacement kinetics, the zinc potential remained unchanged, suggesting that the displacement reaction is negligible. As can be seen in Fig. 1b, the addition of DEA resulted in an extension of this region, along with a more positive zinc immersion potential, contributing to less aggressive behavior. The

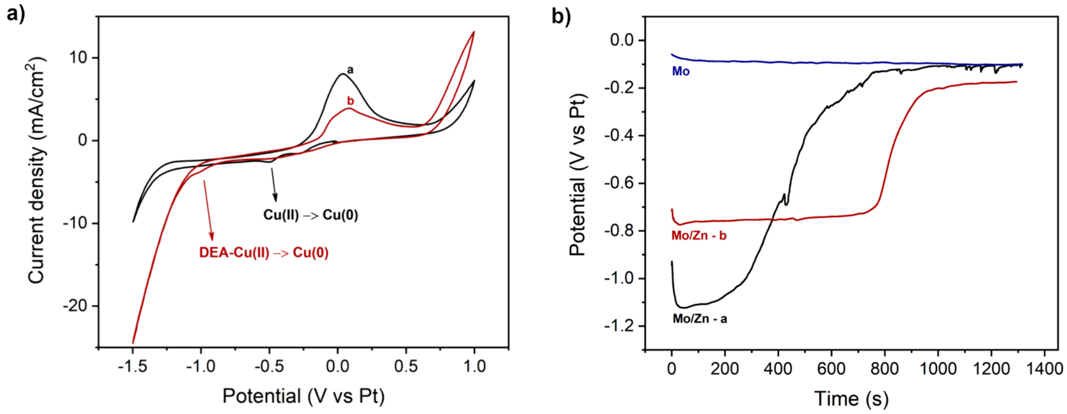

Fig. 1. (a) Cyclic voltammetry (T 70 °C, 20 mV/s) on GC electrode of 0.05 M copper acetate, 1 M sodium acetate in ethylene glycol (curve a) and with the addition of 0.8 M DEA (curve b). (b) Copper displacement investigation (OCV-time graph) of Mo/Zn substrate immersed in a copper 0.05 M copper acetate, 1 M sodium acetate in ethylene glycol (curve a) and with the addition of 0.8 M DEA (curve b) at 70 °C.

complexation with the amine shifted the copper reduction towards more negative potential values (Fig. 1a), with a congruent decrease in the driving force for the displacement reaction. It is also worth noticing that, without DEA, the displacement reaction resulted in a copper layer with poor adhesion that detached during the experiment, exposing the molybdenum underlayer to the solution. The lower displacement kinetics in the presence of DEA resulted in a more compact deposit, with improved adhesion to the substrate. To quantify the displacement reaction rate, the zinc film (Mo/Zn) was immersed in the copper plating solution for 10 s without any applied bias. The resulting ICP-OES analysis detected a minor amount of copper at the sample surface, lower than the 0.16% of the zinc mass (see Supplementary Information). Since the zinc surface was cathodically polarized during deposition, possible displacement could occur only between immersion of the sample and the start of electrodeposition, typically only a few seconds. The displacement reaction thus occurring was therefore negligible, and did not affect the stack composition, with no zinc loss, nor the formation of a copper overlayer.

3.3. Mo/Zn/Cu/Sn stack fabrication and conversion to CZTS

A zinc-sulfate-based commercial solution was employed to guarantee the quality and reproducibility of the zinc layer, with a compact and smooth morphology, in order to study and optimize the copper bath chemistry. The electrochemical characterization of the copper solution demonstrated that the kinetics of the displacement reaction were indeed slow enough to enable the electrochemical apparatus to be set up without damaging the zinc surface (Fig. 1b). SEM micrographs clearly show the high quality of the copper layer, with low surface roughness and a good overall homogeneity (Fig. 2a, c). No bubbles were observed at the substrate surface, meaning that no displacement reaction between Zn and Cu occurred during the apparatus set-up and the deposition, in agreement with the displacement investigation previously presented. A lower deposition current (< -2 mA/cm^2) would indeed result in insufficient cathodic protection of the surface, while at higher cathodic values (> -5 mA/cm^2) the onset for hydrogen evolution, due to EG deprotonation or coordination water electrolysis, would

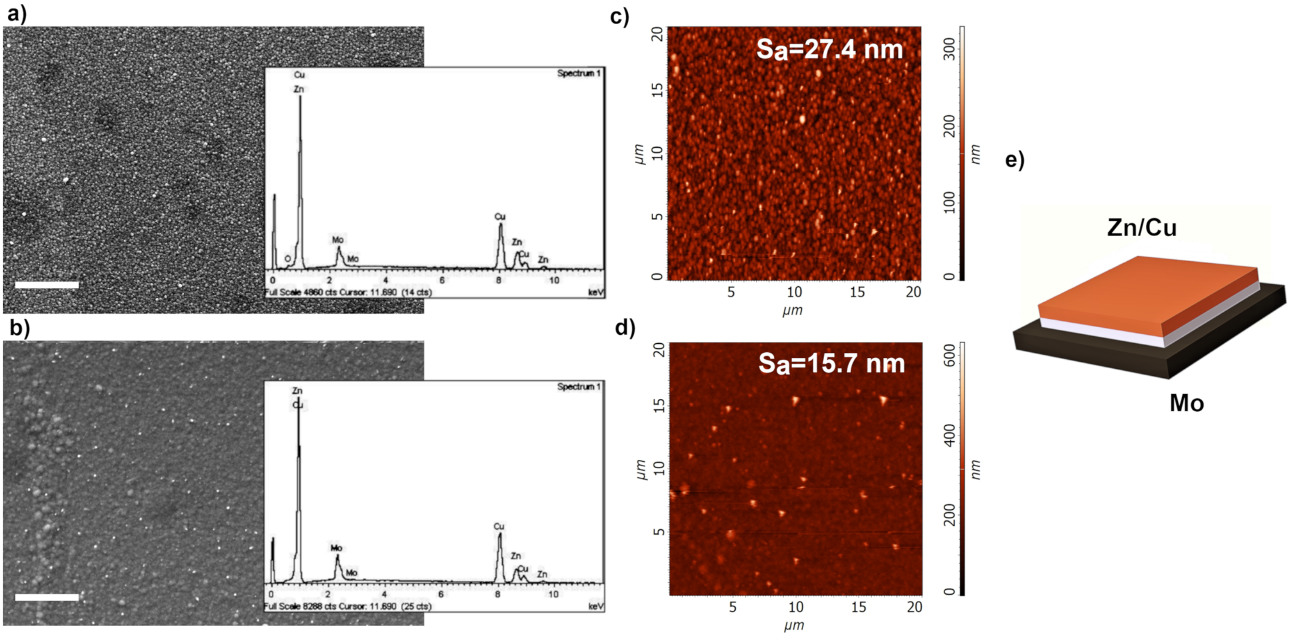

Fig. 2. SEM [scale bar: 5 µm], EDS and AFM analysis of copper layer onto zinc (a, c) −2 mA/cm^2, 70 °C, DEA-free solution. (b, d) −2 mA/cm^2, 70 °C, DEA-containing solution. (e) Graphical representation of the Zn/Cu stack.

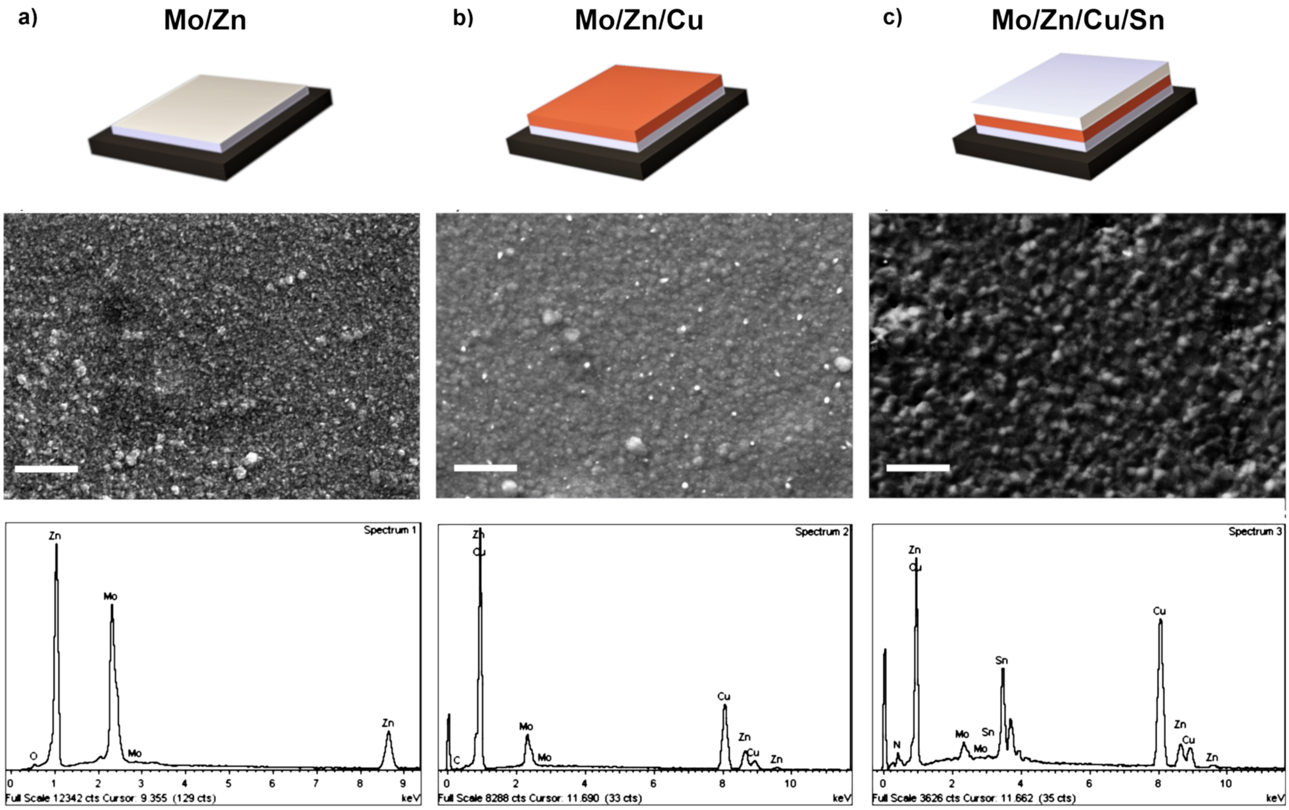

Fig. 3. SEM [scale bar: 3 μm] of the sample surface, EDS and graphical representation of the CZT metallic stack. (a) Mo/Zn; (b) Mo/Zn/Cu; (c) Mo/Zn/Cu/Sn.

result in a lower quality surface morphology, as observed in the preliminary investigation (see Supplementary Information). The morphology of the copper layer showed almost spherical clusters with a diameter of about half a micrometer in a rather sparse arrangement (Fig. 2a, c). Since any porosity in the Cu layer would affect the quality of the top layer, due to the eventual displacement of the uncovered zinc upon immersion in the tin plating bath, the use of an additive was considered. Dimethylamine borane complex [$(CH_3)_2NH{\cdot}BH_3$] was added at a concentration of 0.1 g/L, and produced a significant effect on surface morphology, appearing smoother (average surface roughness $S_a = 15.7$ nm) and with a finer microstructure (Fig. 2b, d), in agreement with the previous report on EG-based solutions [18]. EDS spectra also showed no oxygen or nitrogen/carbon contamination (Fig. 2a, b), indicating that the film was purely metallic and that no organic molecules had been trapped in the film. In the case of a displacement reaction, oxygen is expected to be found since zinc can form an oxide instead of dissolving into the solution.

The good quality of the copper layer was demonstrated using a strongly acidic tin bath, methane sulfonate-based, with no significant damage to the microstructure of the samples (Fig. 3c). The tin layer film showed a compact morphology with a good coverage, in agreement with a previous report using the same bath [9]. However, highly acidic solutions are indeed likely to dissolve copper, exposing the zinc underneath, with a consequent uncontrolled displacement reaction due to the difference in their reduction potentials. It is important to underline that, in the regions where the copper layer is not homogeneous or presents some defects, tin displacement occurs with the consequent appearance of bubbles at the film. EDS analysis showed the high quality of all three layers (Fig. 3a–c), with no oxygen being found. The SEM micrograph and corresponding elemental mapping of the fractured cross section (Fig. 4) showed voids-free interfaces between the different layers, well separated from each other, demonstrating the feasibility of the fabrication route.

Once the stoichiometry of the precursor layer was adjusted to a Zn-

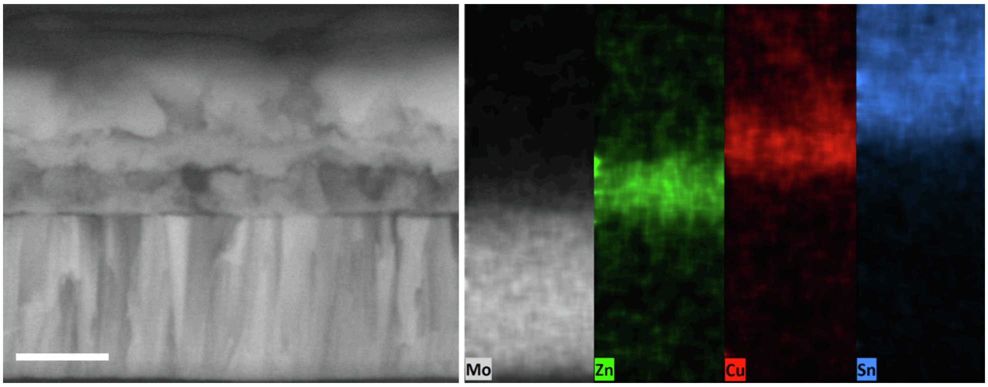

Fig. 4. SEM [scale bar: 500 nm] and elemental mapping of the fractured cross-section of Mo/Zn/Cu/Sn stack.

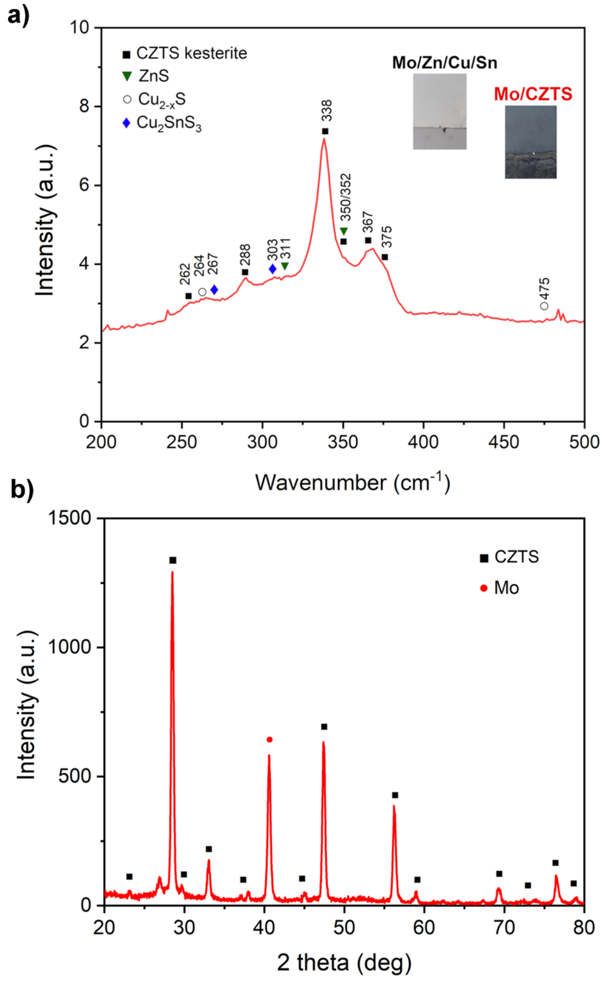

Fig. 5. CZTS film after soft and reactive annealing of the Zn/Cu/Sn stack in a sulfur atmosphere (a) Raman spectrum (b) XRD spectrum.

rich, Cu-poor composition (Zn/Sn ~ 1.1, Cu/(Zn + Sn) ~ 0.85), it was soft annealed in an inert atmosphere (N_2), promoting the formation of intermetallic compounds (Cu_xSn_y, Zn_xCu_y) [19]. Subsequently, the stack of precursors was transformed into CZTS through reactive annealing in a sulfur atmosphere [20] and analyzed by Raman spectroscopy. The analysis showed well-formed kesterite with the minor presence of secondary phases (Fig. 5a), in agreement with the XRD results (Fig. 5b) [21,22].

4. Conclusions

Electrodeposition of a high-quality copper layer on zinc has been successfully achieved through the use of a chloride-free ethylene glycol solution containing diethanolamine. Electrochemical characterization showed how the presence of DEA greatly reduced and minimized the displacement reaction between zinc and copper, making it possible to carry out the electrodeposition. The Zn/Cu/Sn stack, fabricated by means of galvanostatic deposition exploiting zinc and tin acidic solutions, showed a smooth surface finish and a compact morphology. The metallic precursor was reactively annealed and converted into kesterite, proving the suitability of the electrochemical fabrication route to produce CZTS absorber layers for photoconversion devices.

Declaration of Competing Interest

The authors declare that they have no known competing financial interests or personal relationships that could have appeared to influence the work reported in this paper.

Acknowledgement

Authors thank T. Catelani for technical assistance in SEM measurements.

Appendix A. Supplementary data

Supplementary data to this article can be found online at https://doi.org/10.1016/j.elecom.2019.106580.

References

[1] K. Ito, T. Nakazawa, Jpn. J. Appl. Phys. 27 (1988) 2094–2097, https://doi.org/10.1143/JJAP.27.2094.

[2] M.A. Green, E.D. Dunlop, D.H. Levi, J. Hohl-Ebinger, M. Yoshita, A.W.Y. Ho-Baillie, Prog. Photovoltaics Res. Appl. 27 (2019) 565–575, https://doi.org/10.1002/pip.3171.

[3] M. Ravindiran, C. Praveenkumar, Renew. Sustain. Energy Rev. 94 (2018) 317–329, https://doi.org/10.1016/j.rser.2018.06.008.

[4] C. Yan, J. Huang, K. Sun, S. Johnston, Y. Zhang, H. Sun, A. Pu, M. He, F. Liu, K. Eder, L. Yang, J.M. Cairney, N.J. Ekins-Daukes, Z. Hameiri, J.A. Stride, S. Chen, M.A. Green, X. Hao, Nat. Energy 3 (2018) 764–772, https://doi.org/10.1038/s41560-018-0206-0.

[5] S. Ahmed, K.B. Reuter, O. Gunawan, L. Guo, L.T. Romankiw, H. Deligianni, Adv. Energy Mater. 2 (2012) 253–259, https://doi.org/10.1002/aenm.201100526.

[6] D. Colombara, A. Crossay, L. Vauche, S. Jaime, M. Arasimowicz, P.P. Grand, P.J. Dale, Phys. Status Solidi Appl. Mater. Sci. 212 (2015) 88–102, https://doi.org/10.1002/pssa.201431364.

[7] J.J. Scragg, P.J. Dale, L.M. Peter, G. Zoppi, I. Forbes, Phys. Status Solidi Basic Res. 245 (2008) 1772–1778, https://doi.org/10.1002/pssb.200879539.

[8] H. Katagiri, K. Jimbo, M. Tahara, H. Araki, K. Oishi, 1165-M04-01, MRS Proc. 1165 (2009), https://doi.org/10.1557/proc-1165-m04-01.

[9] J.J. Scragg, D.M. Berg, P.J. Dale, J. Electroanal. Chem. 646 (2010) 52–59, https://doi.org/10.1016/j.jelechem.2010.01.008.

[10] E.M. Mkawi, K. Ibrahim, M.K.M. Ali, A.S. Mohamed, Int. J. Electrochem. Sci. 8 (2013) 359–368.

[11] P.K. Sarswat, M. Snure, M.L. Free, A. Tiwari, Thin Solid Films 520 (2012) 1694–1697, https://doi.org/10.1016/j.tsf.2011.07.052.

[12] H. Araki, A. Mikaduki, Y. Kubo, T. Sato, K. Jimbo, W.S. Maw, H. Katagiri, M. Yamazaki, K. Oishi, A. Takeuchi, Thin Solid Films 517 (2008) 1457–1460, https://doi.org/10.1016/j.tsf.2008.09.058.

[13] A. Bakkar, V. Neubert, Electrochem. Commun. 9 (2007) 2428–2435, https://doi.org/10.1016/J.ELECOM.2007.07.010.

[14] M.-J. Deng, P.-C. Lin, J.-K. Chang, J.-M. Chen, K.-T. Lu, Electrochim. Acta 56 (2011) 6071–6077, https://doi.org/10.1016/J.ELECTACTA.2011.04.082.

[15] C.J. Hawkins, D.D. Perrin, J. Chem. Soc. 9 (1962) 1351–1357, https://doi.org/10.1039/JR9620001351.

[16] J.F. Fisher, J.L. Hall, Anal. Chem. 34 (1962) 1094–1098, https://doi.org/10.1021/ac60189a020.

[17] G. Panzeri, D. Muller, A. Accogli, E. Gibertini, E. Mauri, F. Rossi, L. Nobili, L. Magagnin, Electrochim. Acta 296 (2019) 465–472, https://doi.org/10.1016/j.electacta.2018.11.060.

[18] M. Pallaro, F.L. Moretto, G. Panzeri, L. Magagnin, Trans. Inst. Met. Finish. 96 (2018) 265–268, https://doi.org/10.1080/00202967.2018.1507329.

[19] K.V. Gurav, S.M. Pawar, S.W. Shin, M.P. Suryawanshi, G.L. Agawane, P.S. Patil, J.H. Moon, J.H. Yun, J.H. Kim, Appl. Surf. Sci. 283 (2013) 74–80, https://doi.org/10.1016/j.apsusc.2013.06.024.

[20] Y. Ren, N. Ross, J.K. Larsen, K. Rudisch, J.J.S. Scragg, C. Platzer-Björkman, Chem. Mater. 29 (2017) 3713–3722, https://doi.org/10.1021/acs.chemmater.7b00671.

[21] P.A. Fernandes, P.M.P. Salomé, A.F. da Cunha, J. Alloys Compd. 509 (2011) 7600–7606, https://doi.org/10.1016/j.jallcom.2011.04.097.

[22] M. Dimitrievska, A. Fairbrother, X. Fontané, T. Jawhari, V. Izquierdo-Roca, E. Saucedo, A. Pérez-Rodríguez, Appl. Phys. Lett. 104 (2014) 021901, , https://doi.org/10.1063/1.4861593.